Turkish Computational and Theoretical Chemistry

Turkish Comp Theo Chem (TC&TC)

Volume(Issue): 1(1) – Year: 2017 – Pages: 17-26

Received: 21.03.2017 ***Accepted:*** 29.03.2017 *Research Article*

CO_2 transformation on the active site of carbonic anhydrase enzyme leading to formation of H_2CO_3 - A biomimetic model through computational study

Ramasamy SHANMUGAM[a], Arunachalam THAMARAİCHELVAN[b], Balasubramanian VİSWANATHAN[a,1]

[a]National Center for Catalysis Research, Indian Institute of Technology Madras, Chennai, Tamilnadu 600 036, INDIA

[b]Faculty of Allied Health Sciences, Chettinad Academy of Research and Education, Kelambakkam, Tamilnadu 603 103, INDIA

Abstract: Maximizing the utilization of CO_2 through mimicking its activation by nature to form H_2CO_3 is considered and tested. The active site present in the carbonic anhydrase was chosen as the model and various electron releasing and withdrawing substituents were introduced in the imidazole rings to alter the activity of the enzyme model. To compare their activities, the mechanistic pathway was probed for the pure and substituted models employing DFT/B3LYP level of theory. Optimization was performed on structures and the computed energies were used for elucidating the mechanistic pathway. The study reveals that the designed active site model that mimics the nature's process, yields results similar to those observed in nature. The study will help the process of capturing and activation of CO_2 effectively to form H_2CO_3.

Keywords: *CO_2, carbonic anhydrase, DFT, H_2CO_3*

1. Introduction

In the recent years, among the various attractive fields of research, utilization of CO_2 draws more attention due to immense possibility of various products formation [1, 2]. Further, from the point of view of environmental concern, it is the right time to mitigate this global warming greenhouse gas [3]. In order to achieve this, numerous efforts have been undertaken though there is no such process with considerable efficiency.

When nature is looked upon for a solution, it is quite interesting that the enzyme carbonic anhydrase reversibly fixes the CO_2 into bicarbonate [4, 5]. This activity is mainly attributed to the specific active site of the enzyme which is made up of Zn(II) ion surrounded by three histidine units and one water molecule. In reality, the handling of these enzymes at ordinary conditions is difficult. Furthermore, it is not possible to directly use the enzyme as a catalyst for a prolonged time in a reaction.

To overcome hurdles, in handling enzymes, researchers are trying to make the active site containing inorganic complex molecules which is capable of mimicking the catalytic role of an enzyme. These kinds of studies are providing an opportunity to mimic the natural process at the laboratory level [6-8]. Recently, metal organic frame works and transition metal surfaces, exhibited prominent activity towards carbonic acid

[1] Corresponding Author

e-mail: bvnathan@iitm.ac.in

formation reaction [9, 10]. This study prompted the evaluation of such activity by the metal in the enzyme model. In general metals can convert CO_2 to CH_4, CO, HCOOH, CH_3OH, etc. It is desirable to elucidate a new path which can help to transform CO_2 into other value added products to a considerable extent. There are certain metal complexes which effectively catalyze the CO_2 transformation reactions [11-13]. These conclusions revealed that CO_2 could be transformed into various products on carbonic anhydrase. Furthermore, zeolitic imidazole framework (ZIFs) systems, having coordinatively unsaturated metal sites at the end of the corners or surfaces, behave as photocatalysts [14-16] in CO_2 transformation. The above study suggests the view that ZIFs can effectively support the transformation of CO_2.

To achieve effective conversion of CO_2 into H_2CO_3, the active site of the enzyme model was considered. Further, effect of various electron releasing and withdrawing groups was also studied. All these evaluations were carried out using quantum mechanical methods at DFT/B3LYP level.

2. Computational Methods

Geometry optimization and other energy related calculations were performed using Hybrid density functional of B3LYP level of theory. Core electrons in the Zn atom were treated at LANL2DZ level of basis set. Basis set of 6-31g(d) was used for the electrons in all other elements such as C, O, N and H. After initial geometry optimization, stability was further evaluated by calculating the single point energy along with vibrational frequency calculations to find out whether the obtained configurations were in stationary or transition/intermediate states. The interaction between the model and the reactant were evaluated by calculating the binding energy between them. Binding energy (BE), is given by $BE = E_{model+reactant} - E_{model} - E_{reactant}$, where, $E_{model+reactant}$, E_{model} and $E_{reactant}$ are the zero point energy corrected total electronic energy of the model with reactant, pure model and the reactant respectively. The reaction pathway was estimated through determination of the relative Gibbs free energy, $\Delta G = \Sigma G_{products} - \Sigma G_{reactants}$, where, $G_{products}$ and $\Sigma G_{reactants}$ are the zero-point energy corrected Gibbs free energy of the products and reactants respectively at 1 atm pressure and a temperature of 298.15 K. All the electronic structure calculations were carried out using Gaussian 09 software package [17].

3. Results and Discussion

Active site model

Careful analysis of the carbonic anhydrase enzyme reveals that its active site consists of a Zn^{2+} ion which is surrounded by three histidine (substituted imidazole) units and a water molecule to satisfy the valencies of the tetrahedral geometry (Fig.1.a). The active site of the model under study was slightly modified from the original structure in that the histidine unit consists of imidazole and a substituent. In the considered model, the substituent of the imidazole unit was replaced by methyl group. Two-dimensional representation of the modified model is shown in Fig.1. and the schematic representation of the activity of the enzyme is represented in Fig.2.

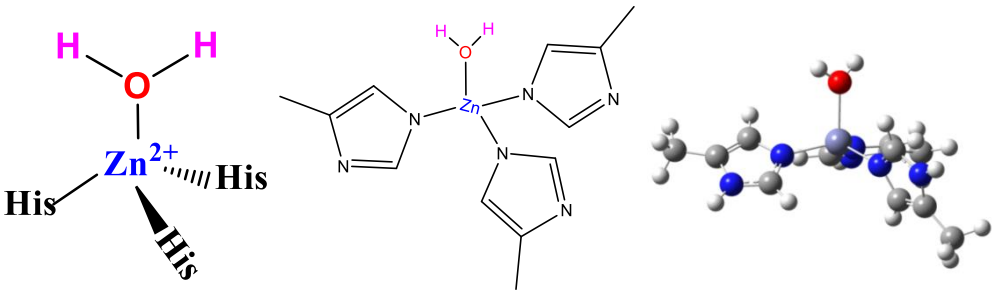

(a) **(b)** **(c)**

Fig. 1. Active site of carbonic anhydrase (a) actual site in enzyme (b) 2-D representation of the model and (c) ball and bond type representation.

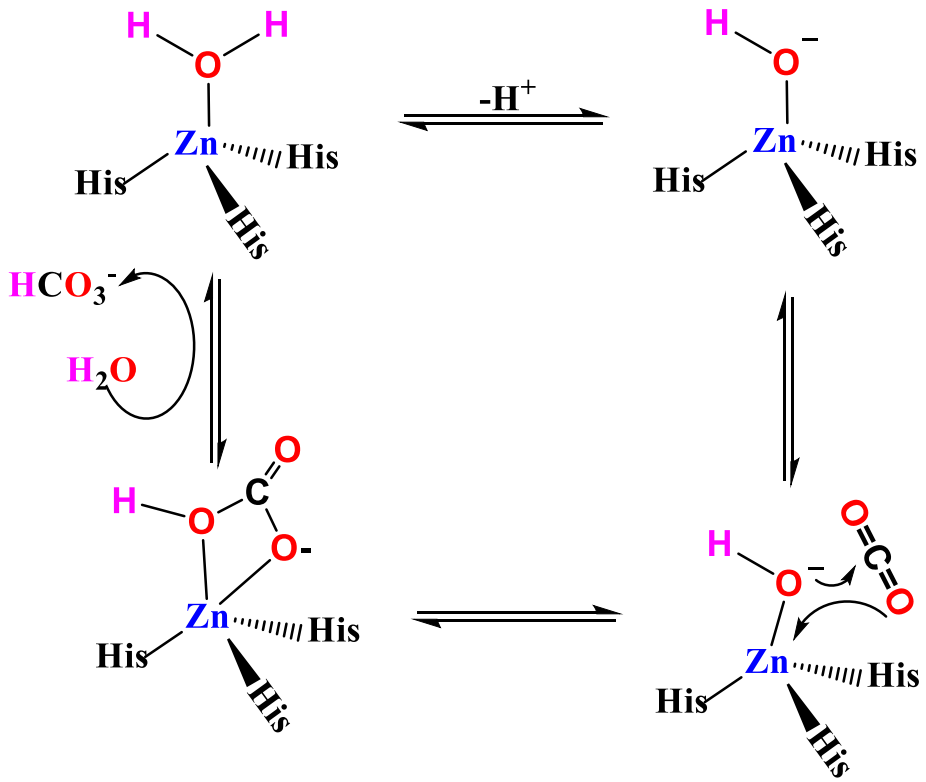

Fig. 2. Schematic representation of the activity of the enzyme in the transformation of CO_2 to H_2CO_3

The structural parameters of the constructed model are presented in Table 1. The values in the tables closely resemble with those found in earlier report [18]. Hence, the present study mainly concentrates on elucidating the nature of CO_2 interaction rather than the structural aspects.

Adsorption of CO_2 on model active site

Prior to the study on the mechanistic pathway of CO_2 transformation, initial assessment of the interaction between CO_2 & H_2O and the active site were evaluated, since, in carbonic anhydrase, all the events take place at the site containing H_2O. This is done with a view to provide clear insight into how the CO_2 gets adsorbed and activated. The possible interaction modes of CO_2 on the active site are as shown in Fig.3.

Table 1. Selected structural parameters of the active site model

Bond length	(Å)	Bond angle	(°)
Zn-O	2.13	O-H-O	106.89
Zn-N1	2.06	O-Zn-N1	100.94
Zn-N2	2.05	O-Zn-N2	103.40
Zn-N3	2.05	O-Zn-N3	107.82
O-H[a]	0.97		
O-H[b]	0.97		

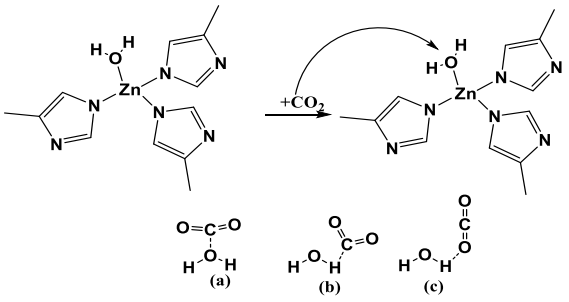

Fig. 3. Possible interaction modes of CO_2 with H_2O in the active site of the chosen model

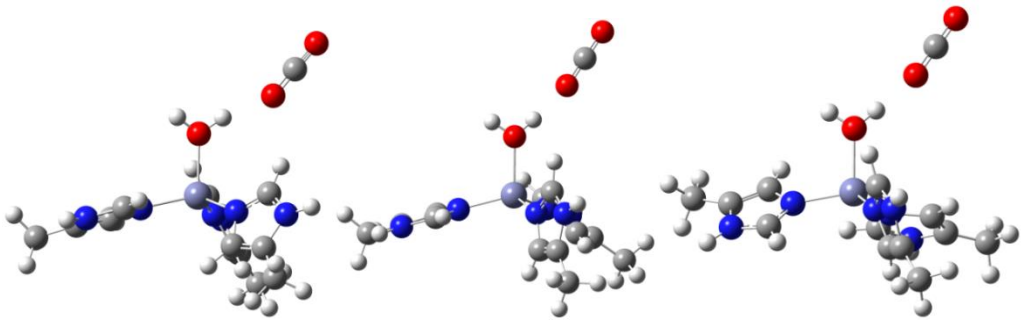

(a) **(b)** **(c)**

Fig. 4. The optimized configurations of the CO_2 interaction modes

During the interaction, three different ways of adsorption are possible for CO_2 with H_2O that are presented in Fig.3(a-c). They are: (a) C of CO_2 interacting with O of H_2O, (b) C of CO_2 orient towards H of H_2O and (c) O of CO_2 approaches towards H of H_2O. These possible interaction modes were initially subjected to geometry optimization, the resultant configurations of which are presented in Fig.4(a-c). From the figure it is clear that, the configurations of CO_2 in all the modes finally retain the linear shape rather than to expected new shape which is evident from the angle of 179.5° for CO_2. The structural parameters and the binding energy of these configurations are listed in Table 2. Further, the CO_2 interacts in all the modes in a similar way through O of CO_2 with H of H_2O at a distance of ~1.85 Å. Although, the angle of O---H-O is 177.44° which is closer to 180° supports the existence of hydrogen bonding.

Deprotonation of H_2O

The carbonic anhydrase reaction pathway is initiated by the removal of H^+ form H_2O via deprotonation step. Although, pure carbonic anhydrase itself is ready to loose H^+, the result of model-CO_2 interaction reveals that one of the oxygens of CO_2 interacts with the H of H_2O to increase the reactivity of the H^+ in comparison to the pure model. Hence, the proton removed during the deprotonation, may also directly migrate to the O of CO_2 to form COOH species. In order to verify this possibility, the COOH species was located at the point where the CO_2 was held physically. On optimization, the proton of COOH was found to migrate to OH forming H_2O and physisorbed CO_2 leading to a structure similar to that obtained in the interaction studies (Fig.4(a)). This result proves that, even though CO_2 may approach H_2O, it won't take up H^+. Hence, it is essential to elucidate the most favorable route for the deprotonation step. Thus, the deprotonation was carried out (i) in the absence of CO_2 and (ii) in presence of CO_2. For both the reactions, the calculated Gibbs free energies were arrived at as -8.02 eV and -7.72 eV respectively. The data reveal that the deprotonation is more favorable in the absence of CO_2, than in the presence of CO_2. Furthermore, the negative sign with higher values suggests that the deprotonation is a spontaneous step. As CO_2 reduces the space available for depronation the free energy decreases in the presence of CO_2. Hence, it may be concluded that the deprotonation step is an independent step.

Table 2. Binding energy (eV) and structural parameters of the CO_2 and H_2O

Optimized configurations	Binding Energy	^{a}H-O (Å)	^{b}H-O (Å)	H-O-H (°)	^{a}O-C (Å)	^{b}O-C (Å)	O-C-O (°)	^{a}O---H^a (Å)
a	-0.29	0.97	0.97	107.42	1.18	1.16	179.48	1.87
b	-0.29	0.98	0.97	106.98	1.18	1.16	179.58	1.85
c	-0.31	0.98	0.97	107.02	1.17	1.15	179.59	1.84

Interaction of CO_2 with OH

In general, the CO_2 directly interacts with OH^- to form HCO_3^- species in the five-coordinated zinc environment of the carbonic anhydrase. To verify this, the CO_2 was placed on OH^- via physisorption and chemisorption modes and then was allowed for relaxation. The result obtained indicates that, configuration of CO_2 in both the modes gets changed and both the final configurations are the same which are presented in Fig.5. The distance between the CO_2 and OH indicates that CO_2 is held by physical adsorption which is further supported by the binding energy value of -0.02 eV.

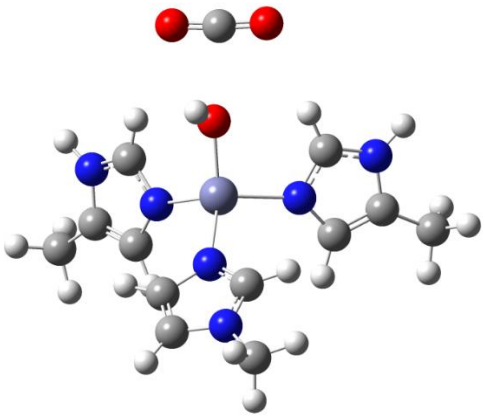

Fig. 5. Optimized structure of CO_2 with deprotanated active site

The active site in the actual enzyme is surrounded by other amino acids and peptide linkages that may facilitate the unusual coordination environment for the reported mechanism. Here, the chosen model does not include the extra environmental interactions. Further, this reactivity is totally different from the proposed usual enzyme activity. However, this study would provide guidelines for the designing of new catalysts to mimic nature's role in CO_2 transformation.

Adsorption of COOH

The dissociated proton, which is present in the medium would be easily added to the CO_2 to form $(COOH)^+$ species which then interacts with the OH^- site in the enzyme model to form H_2CO_3 species. It is interesting to note that in the case of real enzyme, H_2CO_3 is formed by the desorption of HCO_3^- from the active site which further reacts with the H^+ available in the environment. The H_2CO_3 formed from the model active site was allowed for energy minimization and the resultant configuration is presented in Fig.6. The distance of Zn-O was found to be 2.32 Å, which is 0.19 Å higher than that in the pure model. Furthermore, the H_2CO_3 unit does not move far away; but still it is interacting with the active site. This interaction was further probed with the help of binding energies. The value of -0.39 eV is obtained as binding energy for the above interaction. This energy reveals that the molecule is held on to the active site through physical adsorption. Now, it is essential to analyze whether water will be able to replace H_2CO_3 or not. In order to achieve this, the binding energy of H_2O was calculated and the value was -1.31 eV. The binding energy indicates that, H_2O can easily replace the physisorbed H_2CO_3 from the active site.

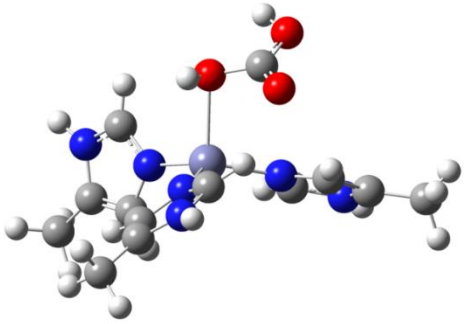

Fig. 6. Optimized structure of H_2CO_3 with the active site

Effect of Substituents in the activity of the Enzyme model

a) Gibbs free energy of formation

As seen from the earlier results, the model mimics the active site activity.

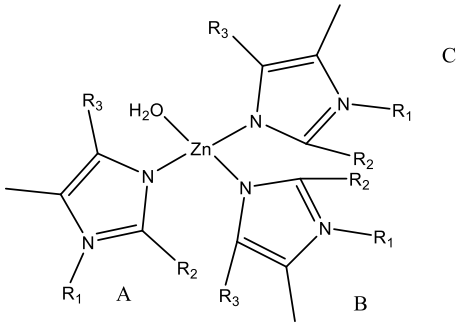

Fig. 7. 2-D Representation of the active site with the various possible substitution sites.

The imidazole moiety was substituted with different R_1, R_2 and R_3 to predict the possible change of the activity of the active site. In general, the activity of any molecule can be easily altered by substituting H of the imidazole by electron releasing and withdrawing groups. The substituents introduced and their complex formation energies are presented in Table 3. While R=Me and Et, they are electron releasing groups and hence release electrons towards the ring.

In turn, the electron density of ligating 'N' of imidazole increases, thus stability of the complexes increases. Where R=NO_2, the electron withdrawing nature of NO_2 depletes electron to make the nitrogen less basic. Hence the complexes formation energy slightly decreases as compared to that of electron releasing groups. NO_2 in position of R_2 makes the steric hindrance without H-bonding, whereas, when it is in R_3, it leads to steric hindrance though H-bonding with H of H_2O may increase the stability of the complex. Hence, NO_2 at R_3 position is more stable than R_2. In the case of halogens, electronegativity plays important role, though the size makes the electron repulsion caucuses the mesomeric effect. This leads to the increase in formation energies in the order, F>Cl>Br. On N-X, resonance effect decreases due to larger & smaller orbital overlap. So, electron density on nitrogen increases. Hence, ligation tendency increases. While comparing the formation energies in N-NO_2 and N-NO, the N-NO has less energy than N-NO_2. This is due to the fact that N-NO has resonance stabilization than N-NO_2, and hence the electrons are not readily available for the effective bonding. Fig. 7**.** Shows the 2D representation of the active site along with the positions of substituents. The electron releasing groups chosen were CH_3- and CH_3CH_2- and electron withdrawing substituents F, Cl, Br, NO_2 and NO groups were considered. Once the substituents were introduced, their thermodynamic Gibbs free energy of formation were calculated which are presented in Table 3.

The Gibbs free energies of formation of the substituted models reveal that all the model sites are thermodynamically favorable and are spontaneous in nature except for the model-19. Since, it has three bigger sized bromine atoms which are present together, the available space in the active site is less due to steric hindrance causing the formation energy as endothermic.

b) Gibbs free energy of deprotonation

The substituent effect on the enzyme model is evaluated by means of predicting the Gibbs free energy of deprotonation step and the second step of the interaction between the CO_2 and OH^- species as these two steps, at the initial stage control the whole of the mechanistic pathway. Hence, Gibbs free energies of the deprotonation have been calculated and are presented in Table 4. All the values have negative sign indicating that the process is thermodynamically feasible. While comparing the deprotonation of substituted models with that of the pure model, most of the models return slightly higher Gibbs free energy than that the pure model.

c) Interaction of CO_2 with OH^-

The interaction of CO_2 with the formed OH^- species was then evaluated. Here, the CO_2 is interacting with the modified models which are similar to the interaction in the pure model. On energy minimization, the calculated binding energy between the model and CO_2 is presented in Table 4. It is quite interesting to see that the values indicate that all the models can up take CO_2 with negative binding energies. Furthermore, the values are almost in the same range except for models 1, 9, 13, 18 & 19. Thus, the CO_2 is held physically as observed in the pure model. However, the models, 1, 9, 13, 18 &19 appear to have higher binding energies compare to other models and hence CO_2 is strongly chemisorbed in them. The chemisorption modes of adsorption of CO_2 on models 1, 9 & 13 are shown in Fig. 8.

Table 3. Various substituents of the model and their Gibbs free energy of formation

S.No (model)	Substituents									ΔG (eV)
	A			B			C			
	R^1	R^2	R^3	R^1	R^2	R^3	R^1	R^2	R^3	
1	CH_3	H	H	H	H	H	H	H	H	-21.50
2	H	H	H	CH_3	H	H	CH_3	H	H	-21.64
3	H	H	H	H	H	H	H	H	H	-21.78
4	ethyl	H	H	H	H	H	H	H	H	-21.60
5	H	H	H	ethyl	H	H	H	H	H	-21.74
6	H	H	H	H	H	H	ethyl	H	H	-21.96
7	ethyl	H	H	H	H	H	ethyl	H	H	-21.78
8	ethyl	H	H	H	H	H	CH_3	H	H	-21.72
9	ethyl	H	H	CH_3	H	H	H	H	H	-21.71
10	ethyl	H	H	ethyl	H	H	H	H	H	-21.76
11	H	F	H	H	H	H	H	H	H	-21.08
12	H	H	H	H	F	H	H	H	H	-21.02
13	H	H	H	H	H	H	H	F	H	-21.05
14	H	F	H	H	F	H	H	F	H	-20.33
15	H	F	H	H	F	H	H	H	H	-20.71
16	H	F	H	H	H	H	H	F	H	-20.71
17	H	H	H	H	F	H	H	F	H	-20.73
18	H	Cl	H	H	Cl	H	H	Cl	H	-18.97
19	H	Br	H	H	Br	H	H	Br	H	6.523
20	H	H	F	H	H	F	H	H	F	-21.47
21	H	H	Cl	H	H	Cl	H	H	Cl	-21.07
22	H	H	NO_2	H	H	NO_2	H	H	NO_2	-19.51
23	H	NO_2	H	H	NO_2	H	H	NO_2	H	-17.11
24	F	H	H	F	H	H	F	H	H	-76.55
25	Cl	H	H	Cl	H	H	Cl	H	H	-75.37
26	Br	H	H	Br	H	H	Br	H	H	-74.76
27	NO	H	H	NO	H	H	NO	H	H	-12.53

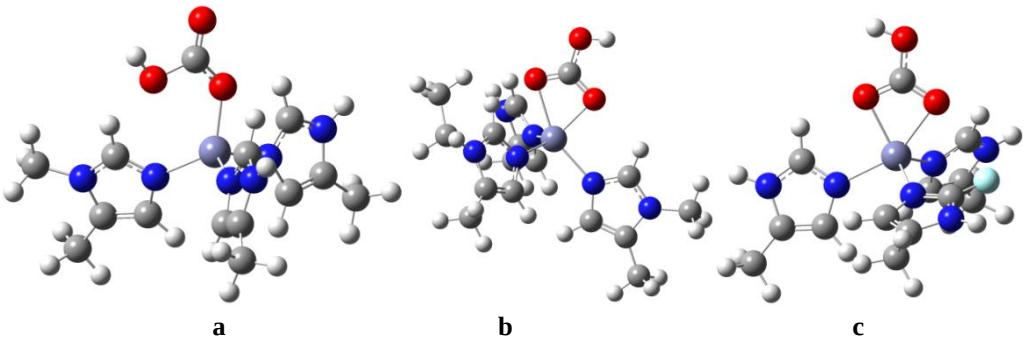

a **b** **c**

Fig.8. Optimized configuration of the CO_2 interaction with OH in various models a=model-1, b=model-9 and c=model-13

A close scrutiny of Fig. 8(a) shows that CO_2 interacts with the H on the OH in the model that migrates to the O of CO_2 to form HCO_3^- leading to a new coordination mode with Zn atom, mono-dentate in model 1 and bridge bi-dentate in models 9 & 13 respectively. This directly reflects in the binding energies. Model-1 has lower binding energy than model-13 and model-9. The Zn-O bond length in model-1 is 1.95 Å, and the average Zn-O bond length in model-9 and model-13 are 2.19 Å and 2.16 Å respectively. The order of stability of the HCO_3^- on these models is: 1<13<9. Although, the models 13 and 9 have similar type of coordination modes resembling that observed in pure model, with the small exception being that the H is on any one of the coordinated oxygens ie., on the free O of HCO_3^-. Hence, it is presumed that the newly obtained configurations may direct the reaction differently. Thus, the following mechanism is proposed in which after the interaction of CO_2 with OH^-, the HCO_3^- formed will be further taking up one H^+ to form *OCOHOH species on the active site. After optimization, the obtained configurations are presented in Fig.9.

Table 4. Structural parameters of H_2O on the modified model, natural bonding orbital charge on the atoms, Gibbs free energy of deprotonation and binding energy(B.E.) of CO_2

				NBO charges |q|			ΔG	CO_2
	O-H4	**O-H3**	**Zn-O**	**O**	**H3**	**H4**	**(eV)**	**B.E. (eV)**
1	0.97	0.97	2.13	-0.979	0.539	0.541	-7.96	-0.58
2	0.97	0.97	2.14	-0.978	0.539	0.539	-7.92	-0.25
3	0.97	0.97	2.14	-0.977	0.539	0.538	-7.84	-0.26
4	0.97	0.97	2.14	-0.979	0.540	0.539	-7.92	-0.25
5	0.97	0.97	2.14	-0.977	0.538	0.538	-7.83	-0.25
6	0.97	0.97	2.14	-0.975	0.537	0.538	-7.74	-0.24
7	0.97	0.97	2.14	-0.817	0.483	0.485	-7.84	-0.26
8	0.97	0.97	2.14	-0.977	0.540	0.538	-7.79	-0.34
9	0.97	0.97	2.14	-0.977	0.539	0.538	-7.88	-1.01
10	0.97	0.97	2.14	-0.977	0.538	0.538	-7.82	-0.23
11	0.97	0.97	2.13	-0.824	0.488	0.479	-7.96	-0.21
12	0.97	0.97	2.13	-0.827	0.479	0.488	-8.09	-0.24
13	0.97	0.97	2.13	-0.982	0.542	0.538	-8.06	-0.92
14	0.97	0.97	2.11	-0.823	0.489	0.482	-7.90	-0.27
15	0.97	0.97	2.11	-0.825	0.488	0.480	-7.98	-0.20
16	0.97	0.97	2.11	-0.824	0.488	0.482	-7.98	-0.09
17	0.97	0.97	2.11	-0.982	0.540	0.543	-7.98	-0.21
18	0.97	0.97	2.10	-0.986	0.543	0.541	-7.76	-0.49
19	0.97	0.97	2.09	-0.985	0.537	0.536	-7.83	-0.49
20	0.97	0.97	2.12	-0.980	0.542	0.542	-8.12	-0.19
21	0.97	0.97	2.11	-0.987	0.539	0.537	-8.10	-0.16
22	0.97	0.98	2.24	-0.967	0.519	0.529	-7.77	-0.28
23	0.97	0.97	2.11	-0.980	0.542	0.539	-7.76	-0.16
24	0.97	0.97	2.12	-0.984	0.544	0.543	-8.41	-0.22
25	0.97	0.97	2.13	-0.982	0.543	0.542	-8.25	-0.22
26	0.97	0.97	2.13	-0.981	0.542	0.541	-8.14	-0.22
27	0.97	0.97	2.12	-0.983	0.543	0.544	-8.26	-0.18

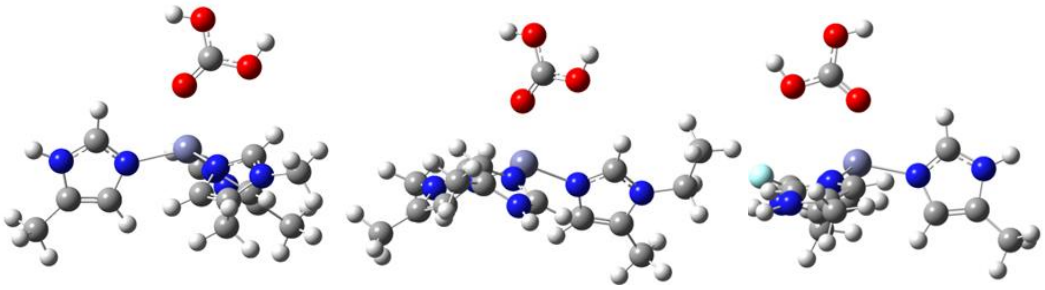

a **b** **c**

Fig.9. Optimized configuration of *OCOHOH species on model a-model-1, b-model-9 and c-model-13.

Fig. 9. reveals that even though, initially the coordination of HCOO may be different, after the uptake of H^+ the bond involved in the coordination gets cleaved before finally forming the H_2CO_3. The formed species then easily gets desorbed from the active site and seems to be simply held physically on. This result indicates that even in the new mode of CO_2 adsorption, it is finally converted easily into the H_2CO_3.

4. Conclusion

An attempt of mimicking the natural activity of carbonic anhydrase towards conversion of CO_2 into H_2CO_3 through simple models, was undertaken to elucidate its activity at DFT/B3LYP level. The results suggest that on the designed model, spontaneous activity could be observed in the original active site. Furthermore, this result supports the observed activity upon addition of ZIFs in photocatalytic reactions, since, the active sites easily capture and activate CO_2.

Acknowledgments

The authors thankful to Department of Science and Technology (DST), India, for setting up the National Centre for Catalysis Research (NCCR), and High Performance Computing Environment (HPCE), Indian Institute of Technology Madras (IITM) for supporting computational facilities. Further R. S. is thankful to Council of Scientific Industrial Research (CSIR) for fellowship., Ref.No. 08/117(0001)-2013-EMR-I.

References

[1] G. Centi, S. Perathoner, Opportunities and prospects in the chemical recycling of carbon dioxide to fuels, Catalysis Today, 148 (2009) 191-205.

[2] A.M. Appel, J.E. Bercaw, A.B. Bocarsly, H. Dobbek, D.L. DuBois, M. Dupuis, J.G. Ferry, E. Fujita, R. Hille, P.J.A. Kenis, C.A. Kerfeld, R.H. Morris, C.H.F. Peden, A.R. Portis, S.W. Ragsdale, T.B. Rauchfuss, J.N.H. Reek, L.C. Seefeldt, R.K. Thauer, G.L. Waldrop, Frontiers, Opportunities, and Challenges in Biochemical and Chemical Catalysis of CO_2 Fixation, Chemical Reviews, 113 (2013) 6621-6658.

[3] M. Aresta, A. Dibenedetto, Utilisation of CO_2 as a chemical feedstock: opportunities and challenges, Dalton transactions, 28 (2007) 2975-2992.

[4] S. Schenk, J. Notni, U. Kohn, K. Wermann, E. Anders, Carbon dioxide and related heterocumulenes at zinc and lithium cations: bioinspired reactions and principles, Dalton transactions, 35 (2006) 4191-4206.

[5] G. Parkin, Synthetic Analogues Relevant to the Structure and Function of Zinc Enzymes, Chemical Reviews, 104 (2004) 699-768.

[6] M. Raynal, P. Ballester, A. Vidal-Ferran, P.W.N.M. van Leeuwen, Supramolecular catalysis. Part 2: artificial enzyme mimics, Chemical Society reviews, 43 (2014) 1734-1787.

[7] T.R. Simmons, G. Berggren, M. Bacchi, M. Fontecave, V. Artero, Mimicking hydrogenases: From biomimetics to artificial enzymes, Coord. Chem. Rev., 270–271 (2014) 127-150.

[8] M.J. Wiester, P.A. Ulmann, C.A. Mirkin, Enzyme Mimics Based Upon Supramolecular Coordination Chemistry, Angewandte Chemie International Edition, 50 (2011) 114-137.

[9] C. Raksakoon, T. Maihom, M. Probst, J. Limtrakul, Hydration of Carbon Dioxide in

Copper-Alkoxide Functionalized Metal–Organic Frameworks: A DFT Study, The Journal of Physical Chemistry C, 119 (2015) 3564-3571.

[10] M. Verma, K.B. Sravan Kumar, P.A. Deshpande, Computational Insights into the Activity of Transition Metals for Biomimetic CO_2 Hydration, The Journal of Physical Chemistry C, 120 (2016) 5577-5584.

[11] G. Jin, C.G. Werncke, Y. Escudié, S. Sabo-Etienne, S. Bontemps, Iron-Catalyzed Reduction of CO_2 into Methylene: Formation of C–N, C–O, and C–C Bonds, Journal of the American Chemical Society, 137 (2015) 9563-9566.

[12] S. Bagherzadeh, N.P. Mankad, Catalyst Control of Selectivity in CO_2 Reduction Using a Tunable Heterobimetallic Effect, Journal of the American Chemical Society, 137 (2015) 10898-10901.

[13] C.C. Chong, R. Kinjo, Hydrophosphination of CO_2 and Subsequent Formate Transfer in the 1,3,2-Diazaphospholene-Catalyzed N-Formylation of Amines, Angewandte Chemie, 127 (2015) 12284-12288

[14] Q. Liu, Z.-X. Low, L. Li, A. Razmjou, K. Wang, J. Yao, H. Wang, ZIF-8/Zn_2GeO_4 nanorods with an enhanced CO_2 adsorption property in an aqueous medium for photocatalytic synthesis of liquid fuel, J. Mater. Chem. A., 1 (2013) 11563-11563.

[15] H.-P. Jing, C.-C. Wang, Y.-W. Zhang, P. Wang, R. Li, Photocatalytic degradation of methylene blue in ZIF-8, RSC Adv., 4 (2014) 54454-54462.

[16] S. Wang, W. Yao, J. Lin, Z. Ding, X. Wang, Cobalt Imidazolate Metal–Organic Frameworks Photosplit CO_2 under Mild Reaction Conditions, Angewandte Chemie International Edition, 53 (2014) 1034-1038.

[17] M.J. Frisch, G.W. Trucks, H.B. Schlegel, G.E. Scuseria, M.A. Robb, J.R. Cheeseman, G. Scalmani, V. Barone, B. Mennucci, G.A. Petersson, H. Nakatsuji, M. Caricato, X. Li, H.P. Hratchian, A.F. Izmaylov, J. Bloino, G. Zheng, J.L. Sonnenberg, M. Hada, M. Ehara, K. Toyota, R. Fukuda, J. Hasegawa, M. Ishida, T. Nakajima, Y. Honda, O. Kitao, H. Nakai, T. Vreven, J.A. Montgomery Jr., J.E. Peralta, F. Ogliaro, M.J. Bearpark, J. Heyd, E.N. Brothers, K.N. Kudin, V.N. Staroverov, R. Kobayashi, J. Normand, K. Raghavachari, A.P. Rendell, J.C. Burant, S.S. Iyengar, J. Tomasi, M. Cossi, N. Rega, N.J. Millam, M. Klene, J.E. Knox, J.B. Cross, V. Bakken, C. Adamo, J. Jaramillo, R. Gomperts, R.E. Stratmann, O. Yazyev, A.J. Austin, R. Cammi, C. Pomelli, J.W. Ochterski, R.L. Martin, K. Morokuma, V.G. Zakrzewski, G.A. Voth, P. Salvador, J.J. Dannenberg, S. Dapprich, A.D. Daniels, Ö. Farkas, J.B. Foresman, J.V. Ortiz, J. Cioslowski, D.J. Fox, Gaussian 09, Gaussian, Inc., Wallingford, CT, USA, 2009, Gaussian Revision C.01.

[18] F. Pannetier, G. Ohanessian, G. Frison, Comparison between [small alpha]- and [small beta]-carbonic anhydrases: can $Zn(His)_3(H_2O)$ and $Zn(His)(Cys).2(H_2O)$ sites lead to equivalent enzymes?, Dalton transactions, 40 (2011) 2696-2698.